International Journal of Emerging Engineering Research and Technology
Volume 2, Issue 3, June 2014, PP 126-144
ISSN 2349-4395 (Print) & ISSN 2349-4409 (Online)

Interleaved DC-DC Converter for Fuel Cell Hybrid Electric Vehicles

K. Suresh

M.Tech Scholor,
EEE DEPT, NBKRIST, Vidyanagar, INDIA
surikanjarappu@gmail.com

B. Sivaprasad Reddy,

Assistant Professor
,EEE DEPT,NBKRIST, Vidyanagar, INDIA
shivareddysmart@gmail.com

Abstract: *Multiphase converter topologies for use in high- performance applications have received increasing interest in re- cent years. This paper proposes a novel multidevice interleaved boost converter (MDIBC) that interfaces the fuel cell with the powertrain of hybrid electric vehicles. In this research, a multi- device structure with interleaved control is proposed to reduce the input current ripples, the output voltage ripples, and the size of passive components with high efficiency compared with the other topologies. In addition, low EMI and low stress in the switches are expected. The proposed dc/dc converter is compared to other con- verter topologies such as conventional boost converter (BC), and two-phase interleaved boost converter (IBC) to verify its dynamic performance. Furthermore, a generalized small-signal model is derived for these dc/dc convertersand which has not been previously discussed. A digital dual-loop control is designed to achieve the proper regulator for the con- verters with fast transient response. The dc/dc converter topolo- gies and their controller are designed and investigated by using MATLAB/Simulink*

Keywords:"Converter losses model, closed-loop control strat- egy, direct digital control (DDC), dc/dc boost converters, fuel cell hybrid electric Vehicles (FCHEVs), generalized small-signal model.

1. INTRODUCTION

FUEL CELL (FC) technologies are expected to become an attractive power source for automotive applications be- cause of their cleanness, high efficiency, and high reliability. Although there are various FC technologies available for use in automotive systems, the polymer electrolyte membrane FC (PEMFC) has been found to be a prime candidate, since PEMFC has high power density with lower operating temperatures when compared to other types of FC systems [1]–[3]. Although FC systems exhibit good power capability during steadystate op- eration, the dynamic response of FCs during transient and in- stantaneous peak power demands is relatively slow. Therefore, the FC system can be hybridized with energy storage systems (ESS) (e.g., batteries or supercapacitors) to improve the per- formance of the FC system during transient and instantaneous peak power demands of a hybrid electric vehicle (HEV) and to recover energy through regenerative braking [1]–[6

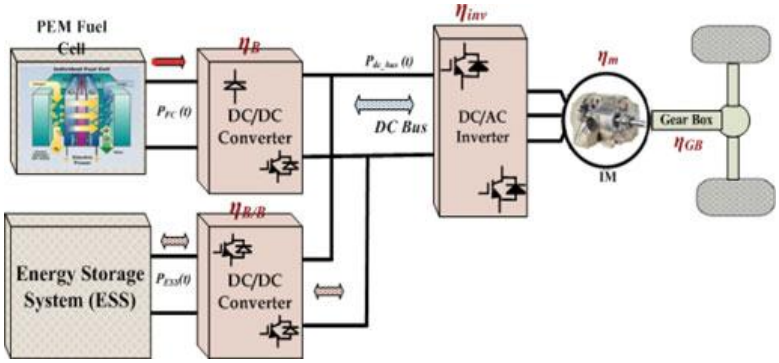

Fig.1. *Block diagram of the FCHEV*

For these applications, a high-power dc/dc converter is a key element that interfaces the FC or ESS with the dc bus in the power train of the HEVs. Therefore, the dc system with multiple dc/dc converters may play an important role in the future power train system. The topology design of dc/dc converters has been documented in many pieces of literature [7]–[13]. In addition, the design of high-power dc/dc converters and their controller play an impor- tant role to control power regulation particularly for a common dc bus. The advantages and disadvantages of serveral topologies of dc/dc converters, based on their component count, are pre- sented and compared in [11]–[14]. Furthermore, for high-power applications, multiphase interleaved converters have been pro- posed for use in electric vehicle applications [15]–[21].

The fuel cell hybrid electric vehicle (FCHEV), as shown in Fig. 1, utilizes an FC as the main power source and the ESS (e.g., batteries and supercapacitors) as the auxiliary power source to assist the propulsion of the vehicle during transients and to recu- perate energy during regenerative braking. In this configuration, the FC is connected to the dc bus through a boost converter, whereas the ESS is connected to the dc bus via a bidirectional dc/dc converter. As was mentioned in much of the literature, the dc/dc converter is one of the most important components in a FC powered system. It allows a desired level of dc voltage to be ob- tained without having to increase the stack size. As a result, this research will focus on a nonisolated dc/dc converter that inter- faces the FC with the powertrain of HEVs. In high-power boost converters, the major design aspect is the selection of the boost inductor and the output capacitor. The major concern is the size, cost, and weight of such a high-power inductor that is perhaps the single heaviest component in the entire dc/dc converter. To reduce the inductor size and weight, a small inductance value is preferred. In addition, the dc/dc converter performance directly influences the characteristics of the FC stack or the ESS (e.g., batteries).

Indeed, the ripple and harmonic content of the current is one of the various phenomena influencing FC lifespan as well as battery lifetime as reported in [6], [10], and [12]. It is clear that the main objective of this research is to minimize inductor size, capacitor, current/voltage ripples, and harmonic content.

In this paper, a novel multi device interleaved boost converter (MDIBC) has been studied and analyzed to reduce the size and weight of the passive components, such as the inductor, capacitor, and input/output electromagnetic interference (EMI) filter. Meanwhile, the input current ripple and output voltage ripple can be minimized with high efficiency and reliability. Further- more, the proposed converter will be compared to other dc/dc converter topologies (e.g., BC, MDBC, and IBC) to investigate its dynamic response. Furthermore, the generalized small-signal model (SSM) and losses model are derived in order to design the appropriate closed-loop control and calculate the efficiency, re- spectively. These models consider the internal resistances of the inductor and capacitor. Moreover, a dual-loop control strategy based on TMS320F2808 DSP has been developed to implement the control strategy for the dc/dc converter. Simulation and ex- perimental results are provided.

2. PROPOSED CONVERTER STRUCTURE

The structure of the MDIBC is depicted in Fig. 2. This con- verter consists of two-phase interleaved with two switches and two diodes connected in parallel per phase. The easy way to reduce the size of the inductor, capacitor, and input/output EMI filter is by increasing the frequency of the inductor current rip- ple and the output voltage ripple. The phase-shift interleaved control is proposed to achieve the control strategy. This con- trol strategy will provide a doubled ripple frequency in inductor current at the same switching frequency, which can contribute to a higher system bandwidth. This bandwidth achieves a fast dynamic response for the converter and reduces the size of the passive components.

In addition, the sequence of the driving signals is very important to providing a doubled ripple frequency in inductor current at the same switching frequency and to achieve the interleaved control between inductors as illustrated in Fig. 3. With the pro- posed control, the switching pattern is shifted by $360^\circ/(n \times m)$, where m is the number of parallel power switches per channel, while n is the number of channels or phases. The input current ripple is $(n \times m)$ times of the switching frequency. Similarly, the output voltage ripple is $(n \times m)$ times of the switching frequency

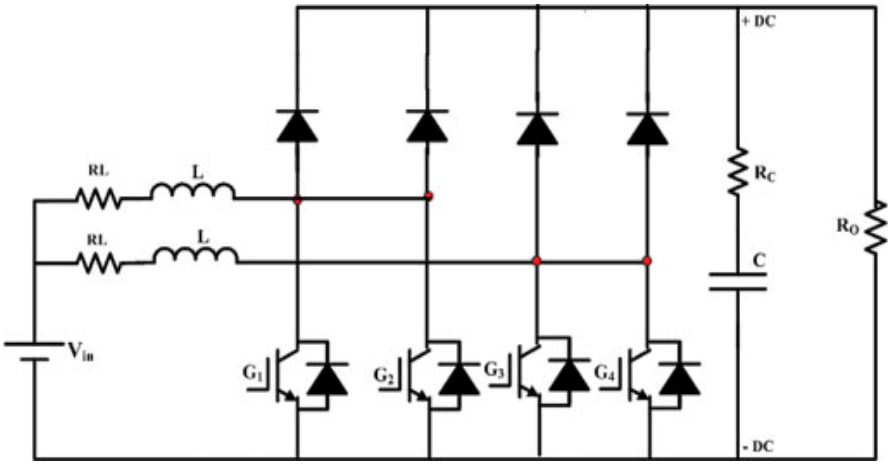

Fig.2. *Structure of the proposed dc/dc converter (MDIBC). (m = 2and n=2).*

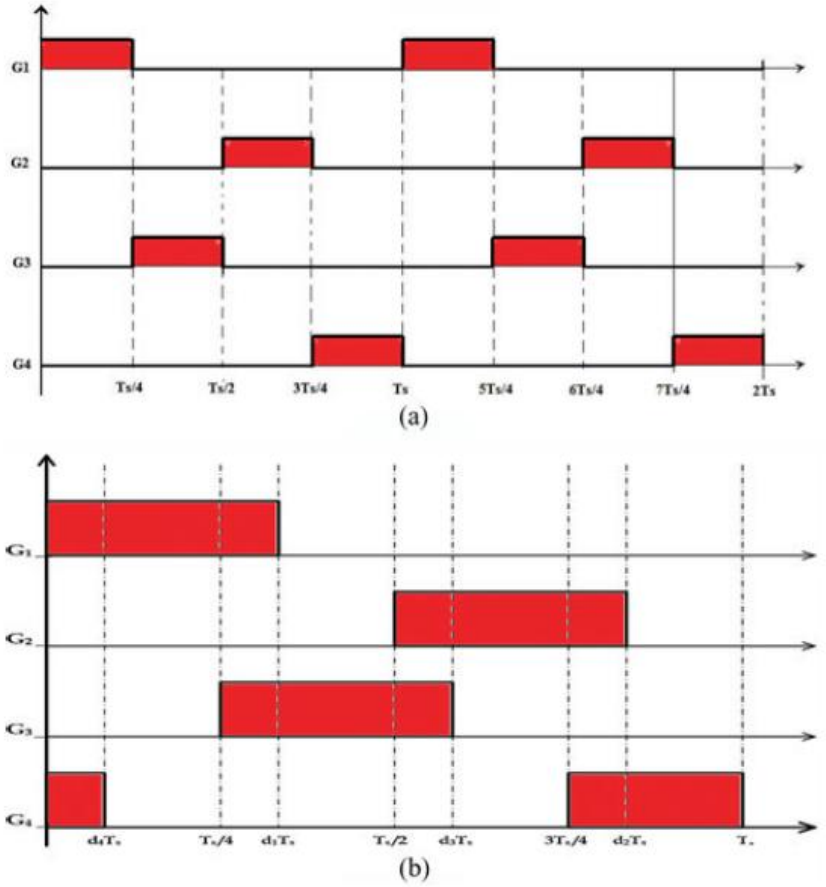

Fig.3. *Sequence of the driving gate signals for switches. (a) d = T_S /4. (b) d≥ T_S /4*

As a result, the size of the passive components will be reduced by *m* times compared with the *n*-phase interleaved dc/dc converters. In this proposed converter structure, *m* is selected to be 2, while *n* is chosen to be 2.

Fig. 3 demonstrates the sequence of the driving signals at different duty cycles. Furthermore, the equivalent circuits of the proposed converter modes for $d > 0.25$ are presented in Fig. 4, where *d* is the duty cycle. It is also assumed that the proposed converter operates in the continuous conduction mode (CCM). The load current is assumed to be rip- ple free. All switches have identical duty cycles which means $d_1 = d_2 = d_3 = d_4 = d$.

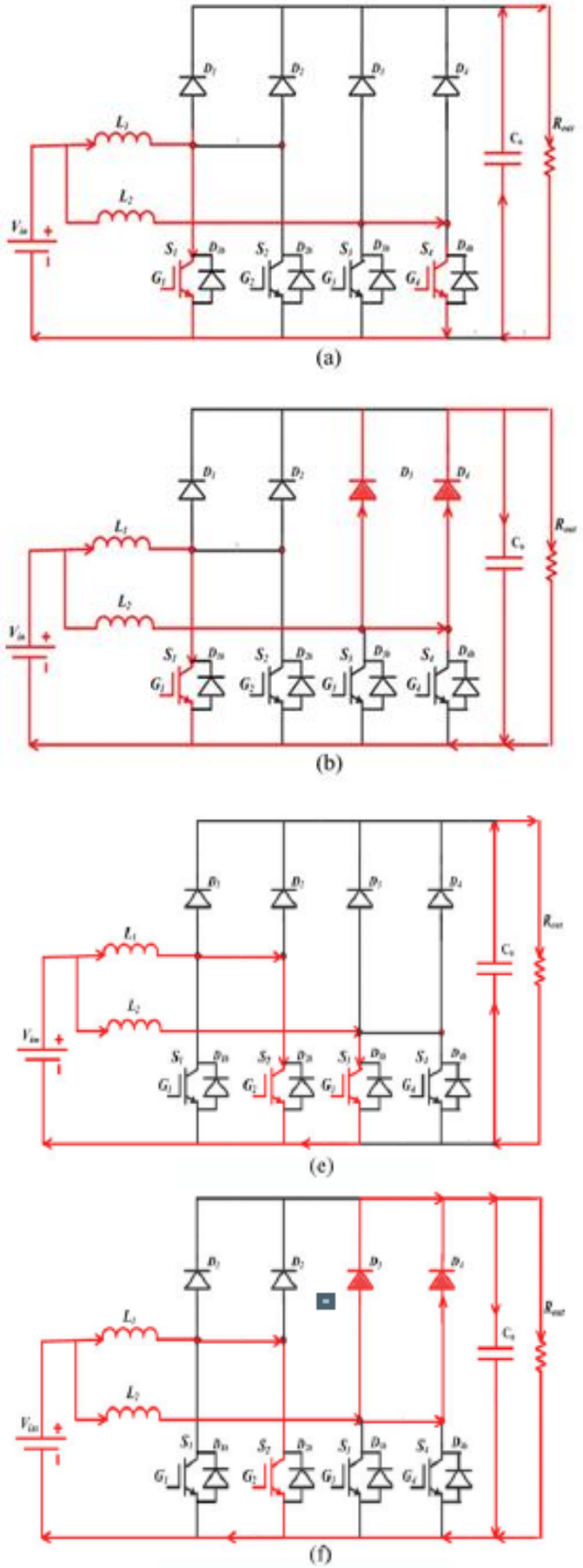

Fig.4. *Equivalent circuits of the proposed converter for d > 0.5. The intervals are mentioned in Fig. 3(b). (a) Mode 1: 0 ≤ t ≤ d4 Ts . (b) Mode 2: d4 Ts ≤ t ≤Ts /4. (c) Mode 3: Ts /4 ≤ t ≤ d1 Ts . (d) Mode 4: d1 Ts ≤ t ≤ Ts /2.*

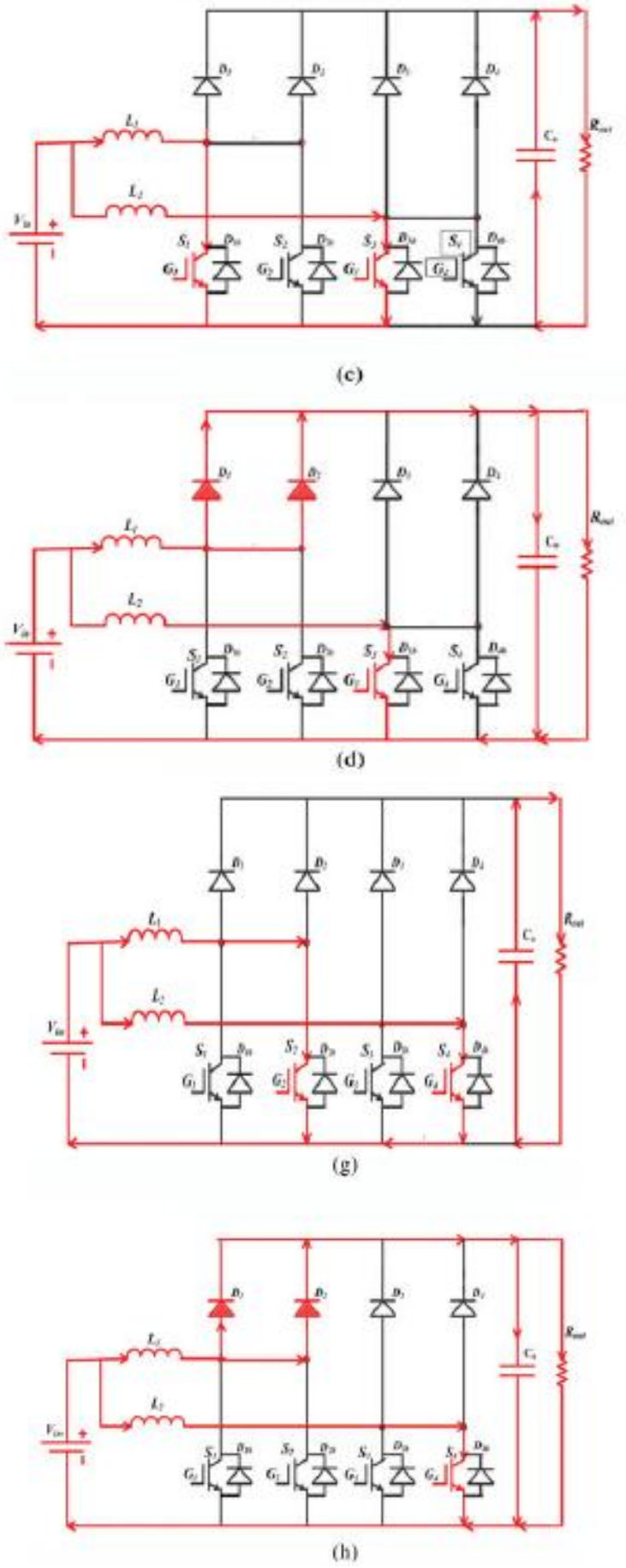

Fig.4.1. *(e) Mode 5: Ts /2 ≤ t ≤ d3 Ts. (f) Mode 6: d3 Ts ≤ t ≤ 3 Ts /4. (g) Mode 7: 3 Ts /4 ≤ t ≤ d2 Ts . (h) Mode 8: d2 Ts ≤ t ≤ Ts*

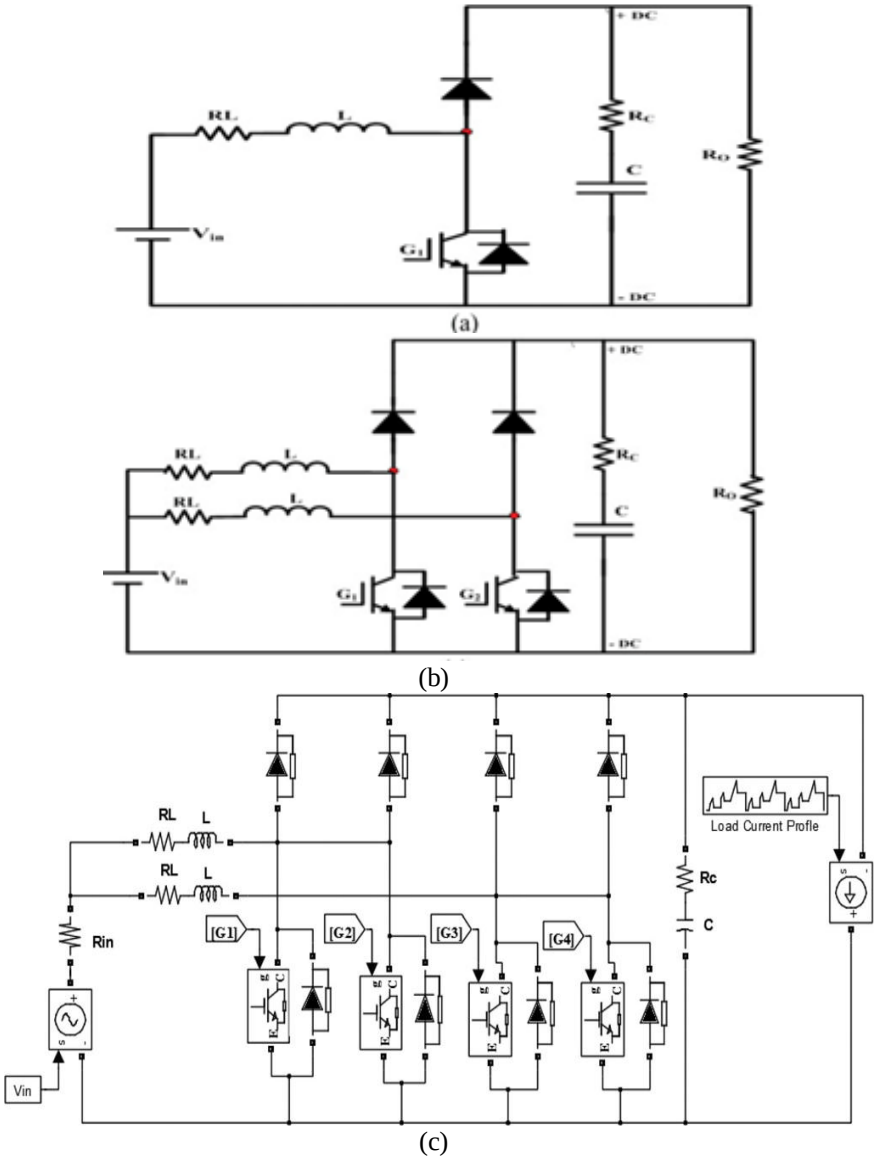

Fig.5 .*DC/DC converter topologies. (a) BC (b) Two-phase IBC (c) MDIBC*

In this research, the proposed converter is compared with three dc/dc converter topologies including conventional boost converter (BC), multidevice boost converter (MDBC), and two- phase interleaved boost converter (IBC) to investigate its per- formance. Fig. 5 presents the configurations of these dc/dc con- verters [6], [14]–[19]

A) Fuel Cell Hybrid Electric Vehicle Structure (FCHEV) For FCHEV has two modes of operation

a) Converting mode of operation

b) Inverting mode of operation

2.1 Converting Mode of Operation

In converting mode of operation fuel cell and battery will produce some amount of voltage and voltage is step up by using multi device boost converter and reduce the voltage ripples , current ripples and size of the passive elements/size of the inductor and capacitor size and battery is used to improve the efficiency of the system.

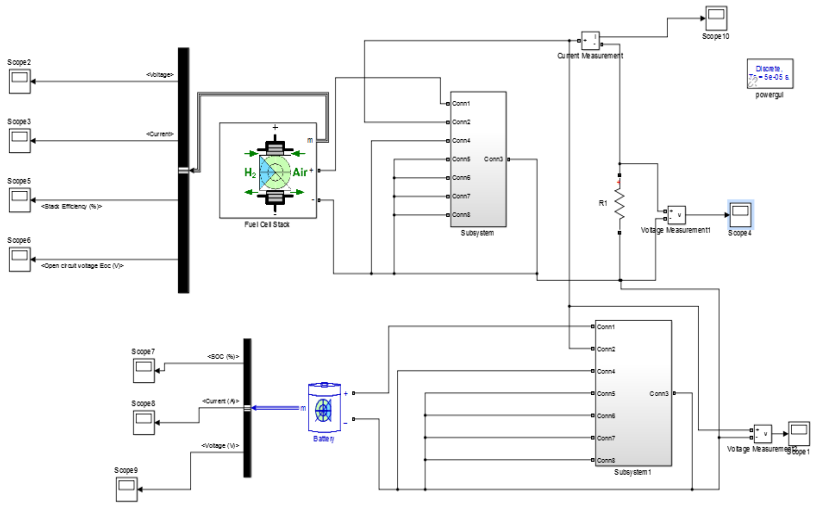

Fig.6. *Converting mode for FCHEV*

2.2 Inverting Mode of Operation

The main feature of the voltage source inverter supply is that the inverter supplying DC voltage is nearly constant, relatively high capacitance capacitor energy storage is built in, to filter the transient load change. To achieve the field oriented control, the switching elements of the inverter constrain voltage to the motor terminals with pulse width modulation control. The higher the switching frequency of the pulse width modulation, the faster and more punctual the achievable field oriented current vector control.

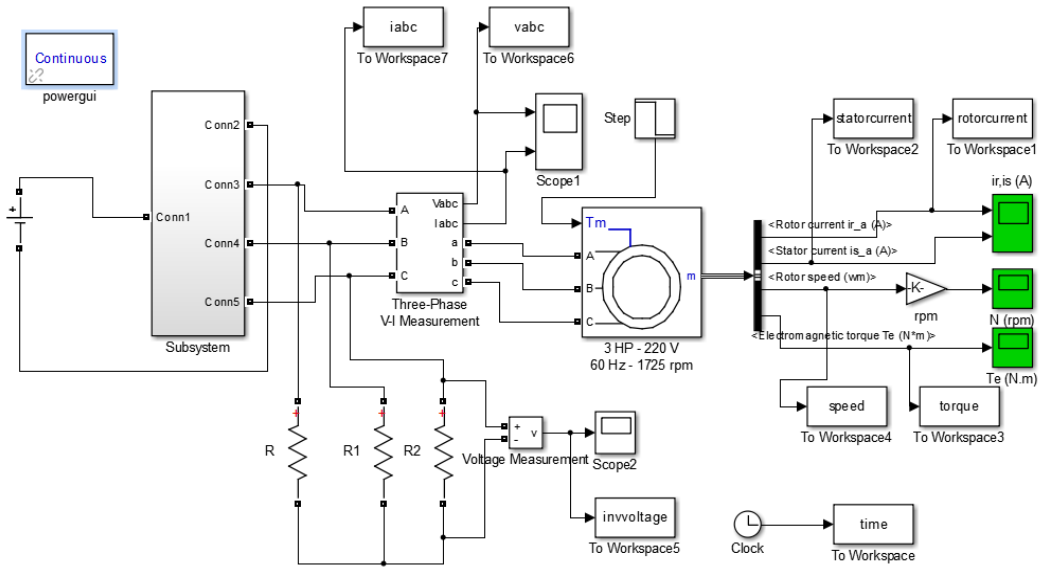

Fig.7. *Inverting mode for FCHEV*

3. GENERALIZED SMALL-SIGNAL MODEL

SSM is a well-known method used to analyze the performance of nonlinear systems such as pulse-width modulated (PWM) dc/dc converters. To obtain a certain performance objective, the SSM is crucial to the design of the closed-loop control for PWM dc/dc converters. The ac-equivalent circuit models have been studied in the literature [22]–[26]. In this paper, a generalized SSM is derived, which has not been discussed previously, to design the appropriate controller using bode diagram. In this paper, the small-signal transfer functions from the duty cycle to the inductor current and from the duty cycle to the output voltage in CCM are derived as follows:

$$G_{vd}(s) = \frac{\hat{\nu}_o(s)}{\hat{d}(s)} = G_{dv}\frac{(1+(s/\omega_{zv1}))(1-(s/\omega_{zv2}))}{\Delta(s)} \quad (1)$$

$$G_{id}(s) = \frac{\hat{i}_L(s)}{\hat{d}(s)} = G_{di}\frac{(1+(s/\omega_{zi}))}{\Delta(s)} \quad (2)$$

$$G_{dv} = \frac{V_o}{(1-D)}\left[\frac{-mR_L + n(1-mD)^2 R_o}{\delta R_L + n(1-mD)^2 R_o}\right] = \frac{V_o}{1-D} \quad (3)$$

$$\omega_{zv1} = \frac{1}{C R_C} \quad (4)$$

$$\omega_{zv2} = \frac{n(1-mD)^2 R_o - mR_L}{mL} \quad (5)$$

$$\Delta(s) = \frac{s^2}{\omega_0^2} + \frac{s}{Q\omega_0} + 1 \quad (6)$$

$$\omega_0 = \sqrt{\frac{\delta R_L + n(1-mD)^2 R_o}{\delta LC(R_o + R_C)}} \quad (7)$$

$$\zeta = \frac{\delta L + C\left(\delta R_L(R_o+R_C) + n(1-mD)^2 R_o R_C\right)}{2\sqrt{\delta LC(R_o+R_C)\left[\delta R_L + n(1-mD)^2 R_o\right]}} \quad (8)$$

$$Q = \frac{1}{2\xi} \text{ and } \delta = \left(\frac{1-mD}{1-D}\right) \quad (9)$$

$$G_{\text{di}} = \frac{V_o(m+\delta)}{\delta R_L + n(1-mD)^2 R_o} \quad (10)$$

$$\omega_{zi} = \frac{1}{C(R_C + (\delta R_o/(m+\delta)))} \quad (11)$$

$$V_o = \frac{V_{\text{in}}}{(1-mD)} \quad (12)$$

$$I_L = \frac{V_o}{n(1-mD)R_o} \quad (13)$$

where V_O is the output voltage, C is the capacitance, L is the inductance, and R_L is the internal resistance of the inductor. R_C is the internal resistance of the capacitor, n is the number of phases, m is the number of parallel switches per phase, V_{in} is the input voltage, D is the duty ratio, and R_O is the resistance of the load. The transfer function (1) is a second-order system, which has two LHP poles: one LHP zero given by (4) and one RHP zero given by (5). The angular corner frequency w_0 and right-half- plane zero w_Z v_2 are the functions of the nominal duty cycle D. In the closed-loop voltage control, the system elements will change as the duty cycle changes, which means that the transfer function will change accordingly. The boost converter under feedback control is a nonlinear function of the duty cycle, which makes the controller design of the boost converter more challenging from the viewpoint of stability and bandwidth [22], [26].

designed to keep a constant bus voltage of 400 V in converter output irrespective of the variations in load and input voltage. The dual-loop control strategy is more efficient than other tech- niques in

achieving a high performance for the PWM boost converter. Fig. 6 shows the schematic diagram of the dual-loop control structure in the s-domain

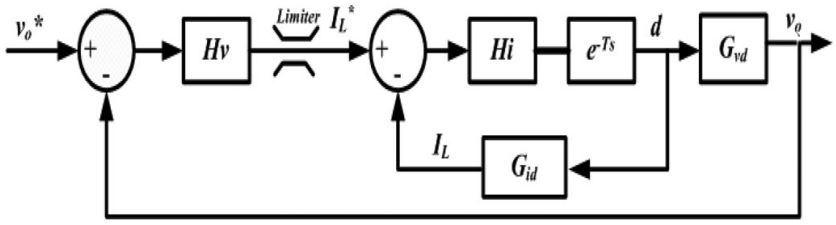

Fig.8. *Schematic diagram of the dual-loop control.*

In general, there are two basic approaches to designing the digital controller for dc/dc PWM converters. The first approach is to design the controller in the s-domain using conventional methods and the resulting controller is transformed into the z-domain using appropriate z transformations. This method is called the digital redesign approach (RDA). The RDA has some drawbacks such as sampling and quantization errors, computational time delay, and discretization effects. The second approach, called direct digital control (DDC), is to directly design the controller in the z-domain itself and thus there is no need for transformation from s- to z-domains. Since the DDC starts with the system discrete transfer functions, it is possible to include the effect of sampling, zero-order-hold (ZOH), and computational time delay effects in order to guarantee the stability of the design [25]–[29].

4. INDUCTION MOTOR

The induction motor has been known since almost the same time as the DC motor, but its role is increased only recently, since the drive technical features have been optimized and secured with inverter supply and field oriented control. The high power switching elements have enabled the development of the inverter technique, and high speed microcontrollers have enabled the development of the complicated control methods.

Field orientation control (FOC) of an induction motor can decouple its torque control from field control. This allows the motor to behave in the same manner as a separately excited dc motor. Extended speed range operation with constant power beyond base speed is accomplished by flux weakening. However, the presence of breakdown torque limits its extended constant power operation as shown in Fig. 12. At the critical speed !mc, the breakdown torque is reached. Any attempt to operate the machine at the maximum current beyond this speed will stall the machine. Generally, for a conventional induction motor, !mc is around two times the synchronous speed !ms. Nevertheless, a properly designed induction motor, e.g., spindle motor, with FOC can achieve a field weakened range of about three to five times its base speed[10].

This approach, however, results in an increased breakdown torque, thereby resulting in over sizing of the motor. A special winding changeover technique of a field orientation controlled induction motor is also reported which demonstrates long field weakening operation [31]. This approach, however, requires winding tap changing and contactors. A contactless control scheme for extending the speed range of a four-pole induction motor was resented in [35]. This scheme uses two inverters, each of half the rated power rating, that, in theory, can extend the constant power operating range to four times the base speed, for a motor, that would otherwise be limited to two times the base speed. It may be mentioned here that the torque control in induction motor is achieved through PWM control of the current. In order to retain the current control capability in the extended speed constant power range, the motor is required to enter the field weakening range before reaching the base speed, so that it has adequate voltage margin to control the current [33]. This would, however, oversize the motor slightly. Current regulation with a synchronous current regulator [36] may be the preferred choice. It can regulate current with a lower voltage margin. The availability of a long field weakened range, obviously, makes the induction very suitable for vehicle application.

Slip-ring induction motors existed also in the past, for example the so-called *Italian system* vehicles powered by three-phase electrification system operating from 1902 to 1976 with rotor resistance

change and mechanical brake. In addition the Ganz-Kandó-type locomotive with phase- and period shifter was a pioneering attempt that was produced with complicated rotating machine converters. The modern induction motor drive technique is a qualitative improvement

The advantage of the induction motor application prevails at *squirrel caged rotor motor* without slip-rings. Comparing with the commutated vehicle drives it possesses robust design, smaller space demand and do not need any maintenance. There are some attempts for water-cooled vehicle drive

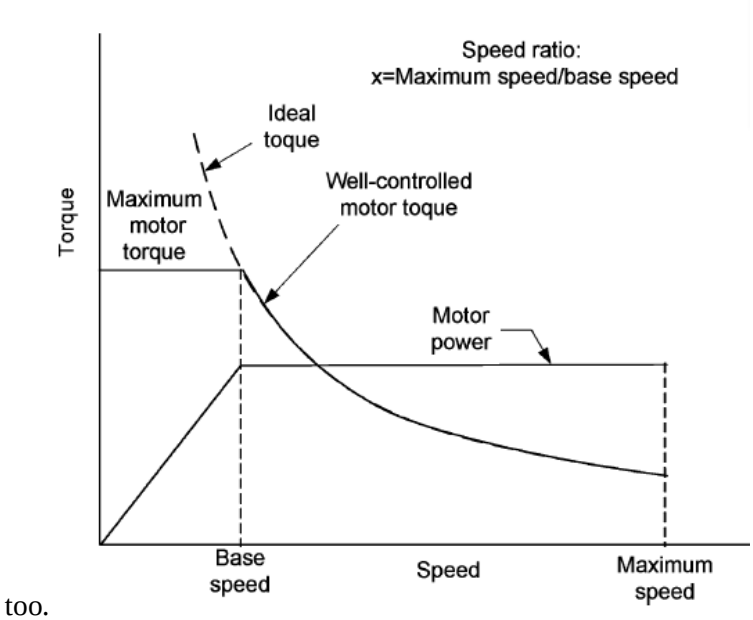

too.

Fig.9. *Ideal torque-speed profile required and that a well-controlled motor can produce*

5. ENERGY STORAGE SYSTEMS

1) Chemical Batteries and Ultra capacitors: Energy storage

is another important component in a hybrid electric drivetrain. It is required to have sufficient peak power and energy capacity to support the operation of the vehicle. At present, almost all the vehicles use chemical batteries as their energy storage.The status of battery systems potentially available for EVs and HEVs [32]. It can be seen that although specific energies are high in advanced batteries, the specific power does not have any significant improvement. About 300 W/kg might be the optimistic estimate. Recently, SAFT has reported their Li-ion high-power and high-energy batteries with about 4000 and 600 W/kg, respectively. However, their practicality and cost reduction in the future need to be further proven.

Ultra capacitor is another candidate as potential energy storage for hybrid vehicles. The ultra capacitor is characterized by high specific power, high efficiency, excellent temperature adaptability, and long service life. However, it has suffered from very limited specific energy. The characteristics of a 42-V ultra capacitor pack specifically listed in Table 3 [38]. Maxwell Technologies [39] have reportedly developed 2700-F ultra capacitors with 2.5-V cell voltage, 2.55-kW/kg specific power, and 3.23-Wh/kg specific energy, respectively. It is believed that the unit power cost of the ultra capacitor is lower than that of batteries. However, due to its low specific energy and dependence of voltage on the state-of-charge, it is difficult to use ultra capacitors alone as the energy storage on hybrid vehicles. The most promising approach is to hybridize the ultra capacitors with other energy storages, such as batteries and flywheel, which will be discussed in the following sections.

2) Hybrid Energy Storage: Compared to ultra capacitors, the chemical has a much higher specific energy but much less specific power. When chemical batteries or an ultra capacitor alone are taken as the energy storage, heavy weight will be unavoidable, because the former needs large weight to meet the power requirement and the latter needs weight to meet the energy requirement. However, when both of them are properly combined, an energy storage with high power and high energy can be obtained. This energy storage is called hybrid energy storage, in which the batteries supply the energy demand and the ultra capacitors supply the power demand. The most straight forward approach is to

directly connect ultra capacitors to batteries as shown in Fig. 14. This configuration has the simplest structure and no control unit is needed. The behavior of the ultracapacitors is more like a current filter, so that high battery peak current is leveled, as shown in Fig. 15.

The leveled battery current by the presence of Ultra capacitors can result in many benefits to the batteries, such as small battery pack, high operating efficiency, easy thermal management, and longer battery life. The lesser variation of terminal voltage can also release the burden of the following power converter. With proper design of all the components, this simply structured energy storage may result in a high power, high energy, and high efficiency energy storage system. Clearly, in the passively connected battery/ultra capacitor system, the power flows between the battery pack a ultra capacitor pack, and when the load cannot be managed, consequently, the high-power characteristic of the ultra capacitors can be fully used. the concept of an actively controlled battery/ultra capacitor system. In this system, a power electronics based power regulator is used to manage the power flow between the battery back, ultra capacitor pack, and the load. Basically, the power conditioning operation can be divided into three different modes [33]: 1) ultra capacitor peaking operation for high power demand (positive and negative); 2) ultra capacitor charging from batteries; and 3) batteries-alone operation. These operation modes are implemented by a central control unit. The central control unit commands the power electronics, according to the control strategy (control logic), and receives signals through current and voltages sensors The control objectives are: 1) to meet the power requirement; 2) to keep the battery current in a preset region; and 3) to keep the battery SOC in its middle region in which the battery efficiencies are usually optimized. This system can potentially fully use the high power property of the ultra capacitors, therefore resulting in a small battery pack. The actively controlled battery current can potentially lead to more efficient battery operation and easier thermal management.

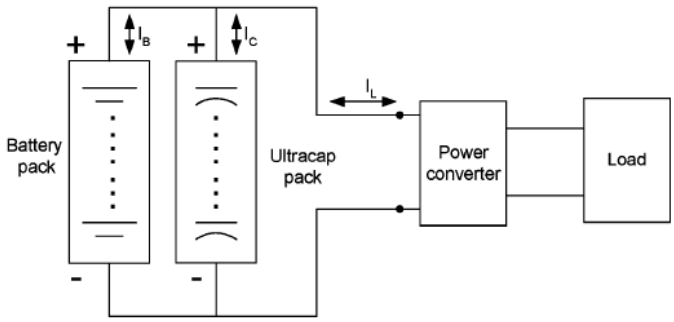

Fig.10. *Passively connected batteries/ultra capacitors system*

Table 1. *Status of Chemical Battery Systems for EV*

	Specific Energy (kW/kg)	Peak Power (W/kg)	Energy Effi.(%)	Cycle life	Cost ($/kW.h)
Acidic Aqueous solution Lead-Acid	35-50	150-400	>80	500-1000	120-150
Alkaline aqueous solution			75	800	250-350
Nickel/cadmium	40-60	80-150	65	1500-2000	200-400
Nickel/Iron	50-60	80-150	70	300	100-300
Nickel/zinc	55-75	170-260	70	750-1200+	200-350
Ni-Metal-Hydride	70-90	200-300	<50	?	?
Aluminum/air	200-300	90	60	500+	50
Iron/air	80-120	90	60	600+	90-120
Zine/air	100-200	30-80			
Flow					
Zinc/Bromine	70-85	90-110	65-75	500-2000	200-250
Vanadium redox	20-30	110	75-85	-	400-450
Molten salt					
Sodium/Sulfur	150-240	230	85	800+	250-450
Sodium/Ni/Cl	90-120	130-160	80	1200+	230-345
Li-ion-sulfur (FeS)	100-130	150-250	80	1000+	110
Organic/lithium					
Lithium-ion	80-130	200-300	>95	1000+	200
Li-ion high power*	85-95	~4000	-	-	-
Li-ion high energy*	135-150	~600	-	-	-

*Reported by SAFT[17]

Table.2. *Dc/Dc Converter Parameters*

Topology	L (μH)	R_L $(m\Omega)$	C (μF)	R_C $(m\Omega)$	$[n\ m]$
*Boost Converter (**BC**)*	750	68	550	0.697	[1 1]
*Multi-Device Boost Converter (**MDBC**)*	375	34	275	1.394	[1 2]
*Interleaved Boost Converter (**IBC**)*	375	34	320	1.15	[2 1]
*Multi-Device Interleaved Boost Converter (**MDIBC**)*	187.5	17	160	2.3	[2 2]

6. SIMULATION RESULTS

In this section, the PWM dc/dc converter topologies are designed and realized by using MATLAB/Simulink in order to

validate the performance of the proposed converter. These simulations are carried out on resistive load with 200V input voltage, 400V output voltage, and 20 kHz switching frequency *Fs* . The comparative study between the BC, MDBC, two-phase IBC, and the proposed converter (MDIBC) is performed under the following converter parameters as mentioned in Table I. Figs. 9 and 10 illustrate the performance of the BC and MDBC, respectively, during load change. Figs. 11 and 12, respectively, show the response of the IBC and the MDIBC during load step. In addition, Figs. 13

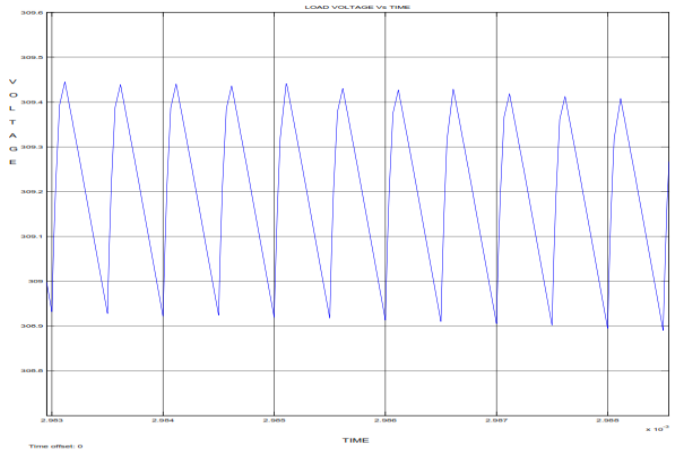

Fig.11.*BC load voltage*

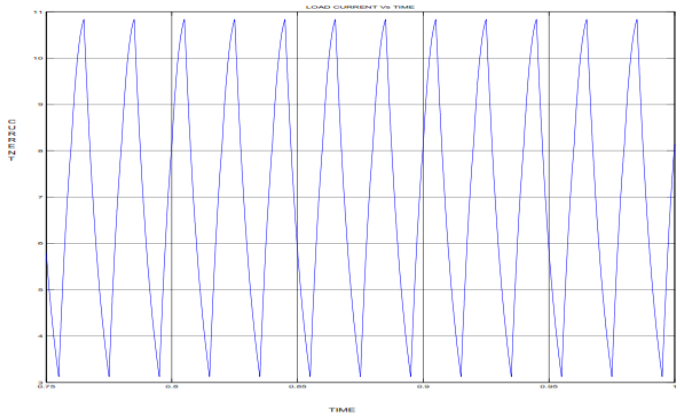

Fig.12. *BC load current*

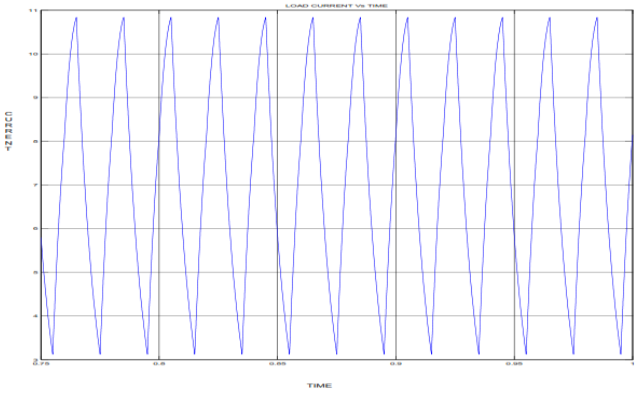

Fig.13. *IBC load current*

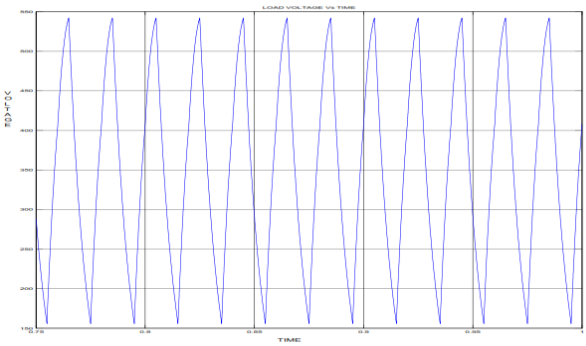

Fig.14. *IBC load voltage*

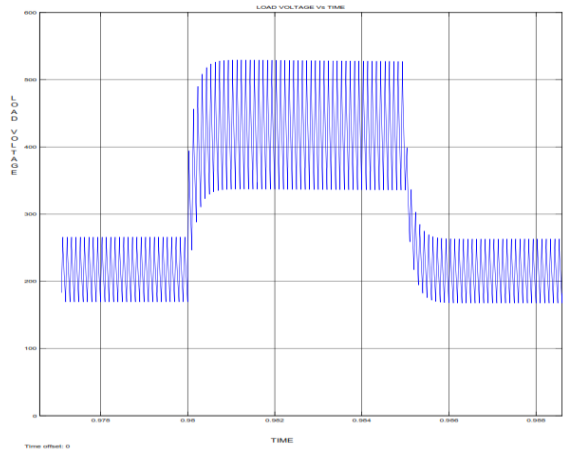

Fig.15. *MDIBC load voltage*

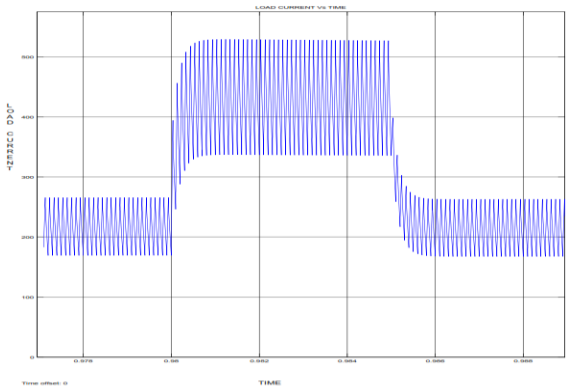

Fig.16. *MDIBC load current*

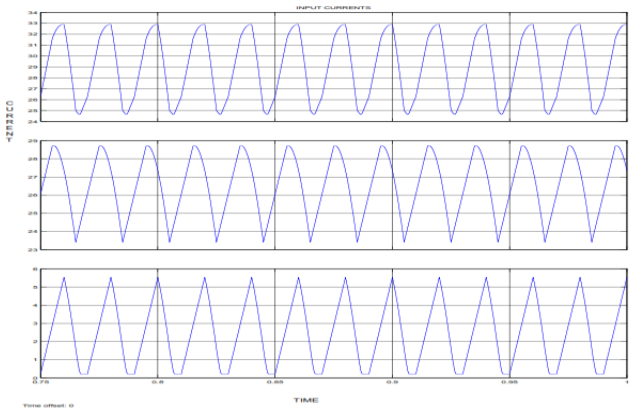

Fig.17. *MDIBC input currents*

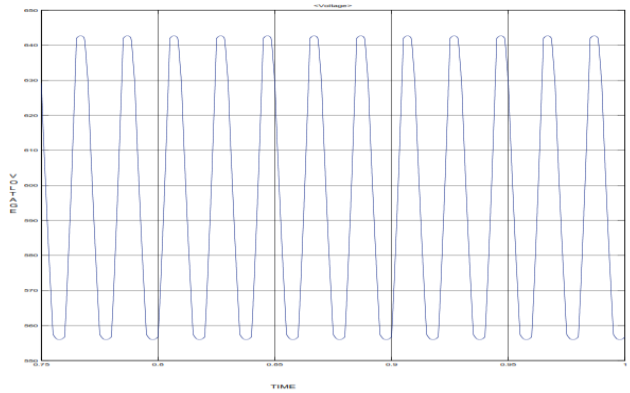

Fig.18. *Fuel cell voltage*

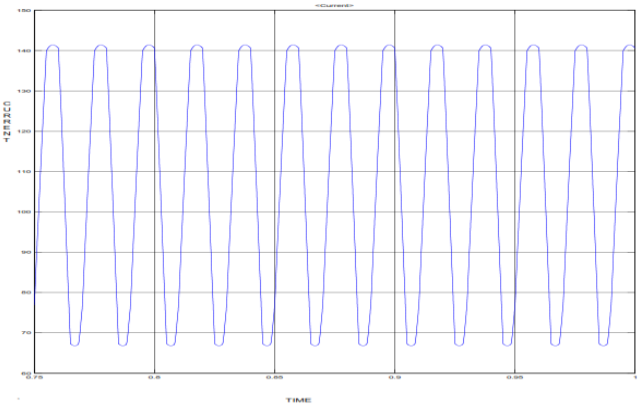

Fig.19. *Fuel cell current*

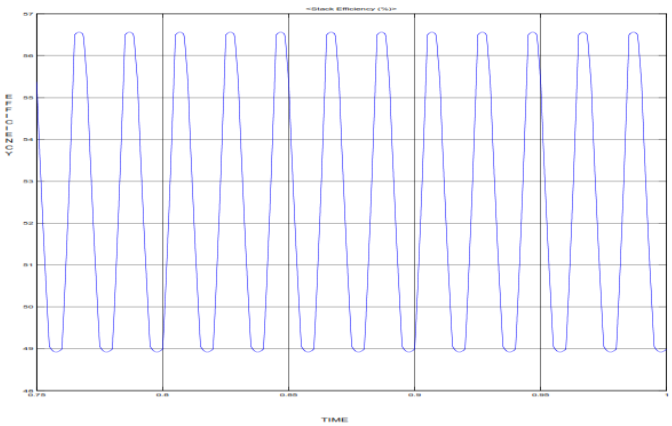

Fig.20. *Fuel cel eficiency*

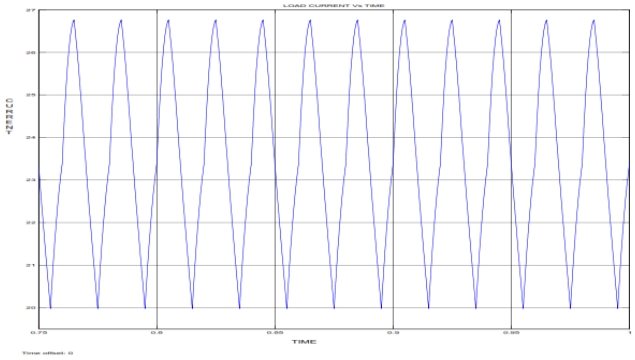

Fig.21. *Load current for converting mode FCHEV*

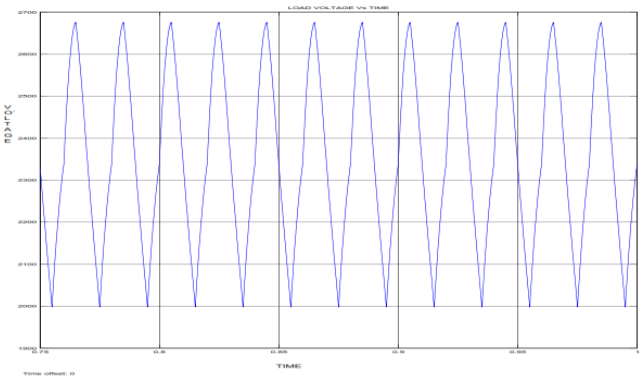

Fig.22 *Load current for converting mode FCHEV*

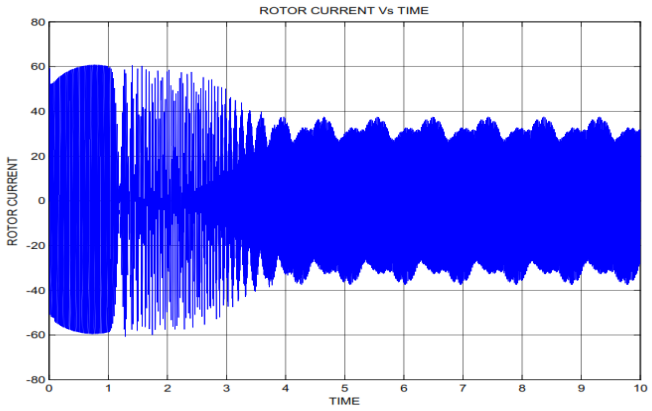

Fig.23. *Rotor current for inverting mode FCHEV*

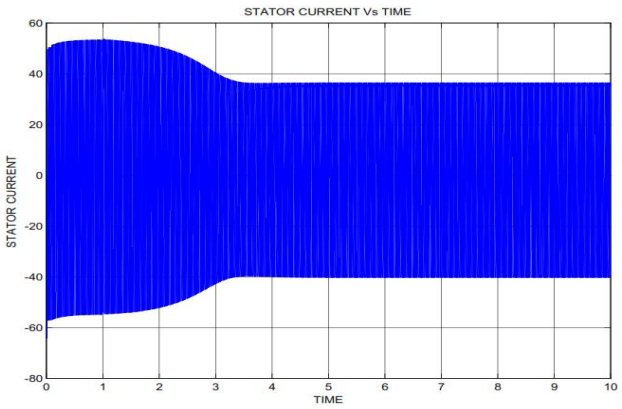

Fig.24. *Stator current for inverting mode FCHEV*

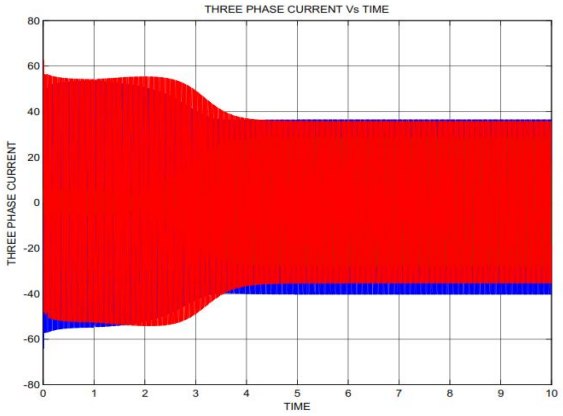

Fig.25. *Three phase currentsfor inverting mode FCHEV*

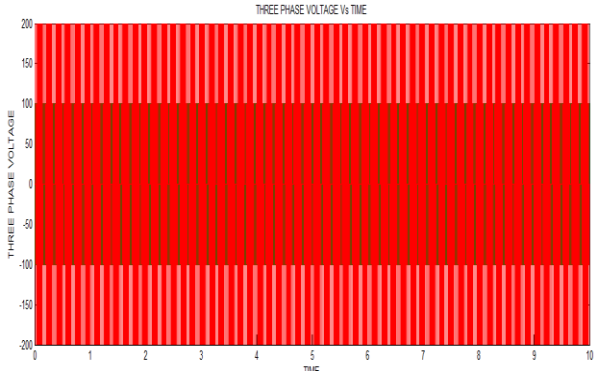

Fig.26. *Three phase voltagesfor inverting mode FCHEV*

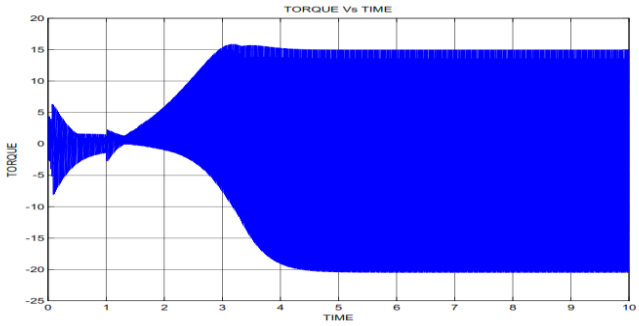

Fig.27. *Torque for inverting mode FCHEV*

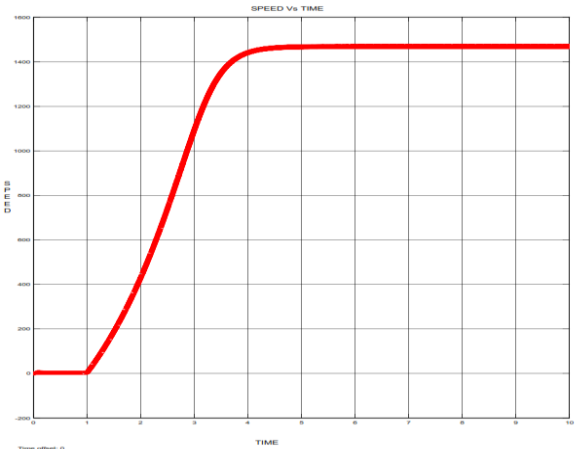

Fig.28. *Speed for inverting mode FCHEV*

7. CONCLUSION

In this project work a new method MDIBC has been proposed for FCHEV system. In order to optimize the drive system the SSM on the ESS model have been derived for the PWM dc to dc converters operating in CCM. The development of MDIBC with PEMFC and ESS to realistic of different drive system like induction motor ,synchronous motor and dc motors and also this method is mainly used for generate electric power to different domestic and industrial purposes. The simulation results have been demonstrated that the inductor and capacitor size of the MDIBC are reduced by two times compare to the IBC. The current and voltage ripples are mitigated by two times compared with IBC topology the proposed converter system to be very promising in high power FC systems to extend their reliability as well as battery system in this MDIBC converter can improve efficiency and reduce the size of the passive components leading to high reliability compared with other dc to dc converter topologies

REFERENCES

[1] K. Jin, X. Ruan, M. Yang, and M. Xu, "A hybrid fuel cell power system,"IEEE Trans. Ind. Electron., vol. 56, no. 4, pp. 1212–1222, Apr. 2009.

[2] A. Emadi, Y. J. Lee, and K. Rajashekara, "Power electronics and motor drives in electric hybrid electric, and plug-in hybrid electric vehicles," IEEE Trans. Ind. Electron., vol. 55, no. 6, pp. 2237–2245, Jun. 2008.

[3] M. Ehsani, Y. Gao, and A. Emadi, Modern Electric, Modern Hybrid, and Fuel Cell Vehicles. New York: Taylor & Francis Group, 2005.

[4] P. Garcia, L. M. Fernandez, C. A. Garcia, and F. Jurado, "Energy man- agement system of fuel-cell-battery hybrid tramway," IEEE Trans. Ind. Electron., vol. 57, no. 12, pp. 4013–4023, Dec. 2010.

[5] J. Van Mierlo, G. Maggetto, and P. Lataire, "Which energy source for road transport in the future? A comparison of battery, hybrid and fuel cell vehicles," Energy Convers. Manag., vol. 47, no. 17, pp. 2748–2760, 2006.

[6] O. Hegazy, J. Van Mierlo, and P. Lataire, "Analysis, control and imple- mentation of a high-power interleaved boost converter for fuel cell hybrid electric vehicle," Int. Rev. Electr. Eng., vol. 6, no. 4, pp. 1739–1747, 2011.

[7] W. Yu, H. Qian, and J.-S. (Jason) Lai, "Design of high-efficiency bidi- rectional DC–DC converter and high-precision efficiency measurement," IEEE Trans. Power Electron., vol. 25, no. 3, pp. 650–658, Mar. 2010.

[8] X. Kong and A. M. Khambadkone, "Analysis and implementation of a high efficiency, interleaved current-fed full bridge converter for fuel cell system," IEEE Trans. Power Electron., vol. 22, no. 2, pp. 543–550, Mar. 2007.

[9] H. Kim, C. Yoon, and S. Choi, "A three-phase zero-voltage and zero- current switchin DC–DC converter for fuel cell applications," IEEE Trans. Power Electron., vol. 25, no. 2, pp. 391–398, Feb. 2010.

[10] M. Al Sakka, J. Van Mierlo, H. Gualous, and P. Lataire, "Comparison of 30 KW DC/DC Converter topologies interfaces for fuel cell in hybrid elec- tric vehicle," in Proc. 13th Eur. Conf. Power Electron. Appl., Barcelona, Spain, Sep. 8–10, 2009.

[11] W. Li and X. He, "Review of nonisolated high-step-up DC/DC converters in photovoltaic grid-connected applications," IEEE Trans. Ind. Electron., vol. 58, no. 4, pp. 1239–1250, Apr. 2011.

[12] M. Kabalo, B. Blunier, D. Bouquain, and A. Miraoui, "State-of-the-art of DC–DC converters for fuel cell vehicles," in Proc. IEEE Vehicle Power and Propulsion Conf., Lille, France, Sep. 1–3, 2010, pp. 1–6.

[13] A. Emadi, S. S. Williamson, and A. Khaligh, "Power electronics intensive solutions for advanced electric, hybrid electric, and fuel cell vehicular power systems," IEEE Trans. Power Electron., vol. 21, no. 3, pp. 567–577, May 2006.

[14] Y.-J. Lee and A. Emadi, "Phase shift switching scheme for DC/DC boost converter with switches in parallel," in Proc. IEEE Vehicle Power Propul- sion Conf., Harbin, China, Sep. 3–5, 2008.

[15] G. A. L. Henn, R. N. A. L. Silva, P. P. Prac¸a, L. H. S. C. Barreto, and D. S. Oliveira, Jr., "Interleaved-boost converter with high voltage gain," IEEE Trans. Power Electron., vol. 25, no. 11, pp. 2753–2761, Nov. 2010.

[16] C. Yoon, J. Kim, and S. Choi, "Multiphase DC–DC converters using a boost-half-bridge cell for high-voltage and high-power applications," IEEE Trans. Power Electron., vol. 26, no. 2, pp. 381–388, Feb. 2011.

[17] Y.-C. Hsieh, T.-C. Hsueh, and H.-C. Yen, "An interleavedboost converter with zero-voltage transition," IEEE Trans.Power Electron., vol. 24, no. 4, pp. 973–978, Apr. 2009.

[18] X. Yang, Y. Ying, and W. Chen, "A novel interleaving control scheme for boost converters operating in critical conduction mode," J. PowerElectron., vol. 10, no. 2, pp. 132–137, Mar. 2010.

[19] H. Xu, X. Wen, and L. Kong, "Dual-phase DC–DC converter in fuel cell electric vehicles," in Proc. 9th IEEE Int. Power Electron. Congr., 2004, pp. 92–97.

[20] T. Reiter, D. Polenov, H. Probstle, and H-.G. Herzog, "PWM dead time op- timization method for automotive multiphase DC/DC-converters," IEEE Trans. Power Electron., vol. 25, no. 6, pp. 1604–1614, Jun. 2010.

[21] P. Thounthong and S. Pierfederici, "A new control law based on the dif- ferential flatness principle for multiphase interleaved DC–DC converter," IEEE Trans. Circuits Syst II, Exp. Briefs, vol. 57, no. 11, pp. 903–907, Nov. 2010.

[22] B. Bryant and M. K. Kazimierczuk, "Small-signal duty cycle to inductor current transfer function for boost PWM DC–DC converter in continuous conduction mode," in Proc. Int. Symp. Circuits Syst., May 23–26, vol. 5, pp. 856–859.

[23] S. K. Mishra, K. Jha, and K. D. T. Ngo, "Dynamic linearizing modulator for large-signal linearization of a boost converter," IEEE Trans. Power Electron., vol. 26, no. 10, pp. 3046–3054, Oct. 2011.

[24] M. K. Kazimierczuk, Pulse-Width Modulated DC–DC Power Converter.Hoboken, NJ: Wiley, 2008.

[25] O. Hegazy, J. Van Mierlo, and P. Lataire, "Control and analysis of an integrated bidirectional DC/AC and DC/DC converters for plug-in hybrid electric vehicle applications," J. Power Electron., vol. 11, no. 4, pp. 408–417, Jul. 2011.

[26] G. Zhou and J. Xu, "Digital average current controlled switching DC–DC converters with single-edge modulation," IEEE Trans. Power Electron., vol. 25, no.3, pp. 786–793, Mar. 2010.

[27] S. Buso and P. Mattavelli, Digital Control in Power Electronics.United States of America: Morgan and Claypool\Publishers, 2006.

[28] Y.-F. Liu, E. Meyer, and X. Liu, "Recent developments in digital control strategies for DC/DC switching power converters," IEEE Trans. Power Electron., vol. 24, no. 11, pp. 2567–2577, Nov. 2009.

[29] S. Choudhury, "Designing a TMS320F280x based digitally controlled DC–DC switching power supply," Texas Instruments, TX, Appl. Rep. SPRAAB3, pp. 1–5, July 2005.

[30] Metglas, Inc. (2008) Inductor Cores, Power lite Technical Bulletin, PLC09302008. [Online]. Available: http://www.metglas.com.

[31] M. Ehsani, Y. Gao, and K. L. Butler, B Application of electrically peaking hybrid (ELPH) propulsion system to a full size passenger car with simulated design verification,'' IEEE Trans. Vehicular Technol., vol. 40, no. 6, Nov. 1999.

[32] C. C. Chan and K. T. Chau, Modern Electric Vehicle Technology. New York: Oxford Univ. Press, 2001.

[33] J. Y. Wong, Theory of Ground Vehicle. New York: Wiley, 1978, pp. 132–133.

[34] M. Ehsani, Y. Gao, and S. Gay, B Characterization of electric motor drives for traction applications,[in Proc. Industrial Electronics Society, IECON '03, Nov. 2–6, 2003, pp. 891–896.

[35] Z. Rahman, K. L. Butler, and M. Ehsani, BEffect of extended-speed, constant-power operation of electric drives on the design and performance of EV propulsion system,[presented at the SAE Future Car Congr., Apr. 2000, 2001-01-0699.

[36] K. M. Rahman and M. Ehsani, BPerformance analysis of electric motor drives for electric and hybrid electric vehicle application,'' Power Electron. Transportation, pp. 49–56, 1996.

[37] C. C. Chen and K. T. Chau, Modern Electric Vehicle Technology. New York: Oxford Univ. Press, 2001, pp. 122–133.

[38] C. C. Chan, K. T. Jiang, J. Z. Xia, W. Zhu, and R. Zhang, B Novel permanent magnet motor drive for electric vehicles,'' IEEE Trans. Indust. Electron., vol. 43, no. 2, Apr. 1996. [36] K. M. Rahman and M. Ehsani, BPerformance analysis of electric motor drives for electric and hybrid electric vehicle application,'' Power Electron. Transportation, pp. 49–56, 1996.

[39] C. C. Chen and K. T. Chau, Modern Electric Vehicle Technology. New York: Oxford Univ. Press, 2001, pp. 122–133.

[40] C. C. Chan, K. T. Jiang, J. Z. Xia, W. Zhu, and R. Zhang, B Novel permanent magnet motor drive for electric vehicles,'' IEEE Trans. Indust. Electron., vol. 43, no. 2, Apr. 1996.

[41] B. P. Ferraris and M. Lazzari, BA new design criteria for spindle induction motors controlled by field orientated technique,'' Electric Machine Power Syst., vol. 21, pp. 171–182, 1993.

[42] T. Kume, T. Iwakane, T. Yoshida, and I. Nagai, BA wide constant power range vector-controlled ac motor drive using winding changeover technique,'' IEEE Trans. Industry Applic., vol. 27, no. 5, pp. 934–939, Sept./Oct. 1991.

[43] Osama and T. A. Lipo, BA new inverter control scheme for induction motor drives requiring speed range,[in

[44] B. P. Ferraris and M. Lazzari, BA new design criteria for spindle induction motors controlled by field orientated technique,'' Electric Machine Power Syst., vol. 21, pp. 171–182, 1993.

[45] T. Kume, T. Iwakane, T. Yoshida, and I. Nagai, BA wide constant power range vector-controlled ac motor drive using winding changeover technique,'' IEEE Trans. Industry Applic., vol. 27, no. 5, pp. 934–939, Sept./Oct. 1991.

[46] Osama and T. A. Lipo, BA new inverter control scheme for induction motor drives requiring speed range.